Increasing the Dynamic Pressure Capability of the NASA Langley/ODU 6-inch MSBS

Mark Schoenenberger[1], David Cox[2], Eli Shellabarger[1]
[1]Atmospheric Flight and Entry Systems Branch
[2]Dynamic Systems and Control Branch
NASA Langley Research Center, Hampton, VA, USA
Hisham Shehata[3]
[3]Analytical Mechanics Associates
Hampton, VA, USA
Colin Britcher[4], Brendan McGovern[4]
[4]Department of Mechanical and Aerospace Engineering
Old Dominion University, Norfolk, VA, USA

ABSTRACT

The 6-inch NASA/ODU Magnetic Suspension and Balance System (MSBS) has been configured for dynamic stability testing of blunt-body atmospheric entry capsules. Tests have been successfully accomplished in the low-speed, open-circuit wind tunnel, at speeds up to around 40 m/s. The wind tunnel is designed to reach around 150 m/s, resulting in dynamic pressures comparable to those projected to arise in a future supersonic MSBS facility. Extensive system upgrades are being undertaken to permit testing at higher speeds/dynamic pressures, including control system enhancements, revised position and attitude sensing, and activation of additional electromagnets in the existing array. This paper will review recent progress in all these areas.

1. Introduction

The magnitude of the force per unit volume acting on an MSBS model's magnetic core has practical limitations. Hence there is interest in restricting the dynamic pressure ("q") in wind tunnels equipped with MSBSs and a rule-of-thumb for realistic values can be established based on prior experience. Several early MSBSs were configured for testing at supersonic or hypersonic Mach numbers, although the electromagnetic configurations featured axial magnetization of relatively slender models, distinct from the current configuration at NASA Langley. A few examples are given below.

• The RAE Farnborough 18 cm MSBS [1] operated in a hypersonic wind tunnel, nominal Mach number 8.5. Stagnation pressures around 3.5 MPa resulted in dynamic pressures around 12 kPa.

• The MIT low-speed wind tunnel was configured to be capable of generating dynamic pressures similar to those expected in supersonic operation, around 15 kPa. An early MIT MSBS design was used at Mach 4.28 with q around 12 kPa [2].

• The Tohoku University/Institute for Fluid Science 0.1m MSBS has been operated in an indraft wind tunnel with maximum q estimated as around 35 kPa [3]

• The long-term objective of the current project is to develop an all-new MSBS for a supersonic wind tunnel at NASA Glenn Research center. The target Mach number is 2.5, with a dynamic pressure of 13 kPa, although operation at higher or lower q values is possible [4].

2. The NASA/ODU 6-inch MSBS

Originally developed by MIT for NASA, the system was a one-of-a-kind design with an array of water-cooled electromagnets configured to provide natural separation between field and field gradient components. A unique position and attitude sensing system was chosen – the Electromagnetic Position Sensor (EPS), which functions as a multi-degree-of-freedom linear variable differential transformer. Aerodynamic models were typically slender along the wind axis with an axially magnetized soft iron core [5].

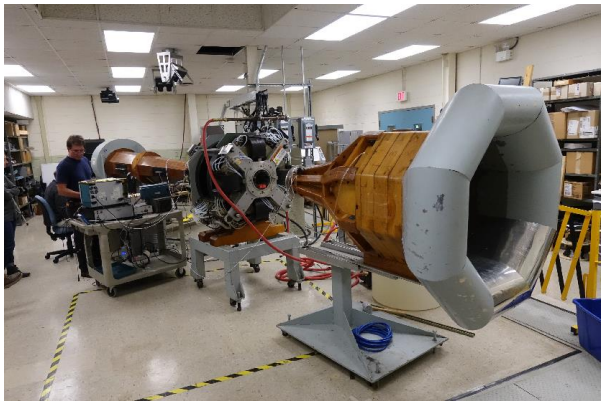

Figure 1 NASA/ODU 6-inch MSBS

2.1 Prior Use at NASA Langley

The recent system baseline at NASA LaRC is a novel configuration with transverse magnetization [6], Three degrees-of-freedom (x, y, z) are controlled and two (pitch and roll) are passively stable. The magnetization direction of the magnetic core is along the yaw axis, resulting in a free-to-yaw configuration. For the present application, all electromagnets have been reassigned from their original functions, with some rewiring to change the field components generated. A summary of the changes is shown in Table 1 below, with the associated geometry shown in Figure 2. Note that the original axial magnetizing field is no longer required, instead a steady vertical field is used to establish the alignment of the magnetization axis. Other hardware upgrades include Performance Controls GA-301 amplifiers, used singularly, or as parallel pairs or triples depending on current requirement.

Corresponding author: Colin Britcher
E-mail address: britcher@aero.odu.edu

Table 1 Field components and functions

Original MIT configuration (M_x)						
Field	B_x	B_y	B_z	B_{xx}	B_{xy}	B_{xz}
Coils	MAG	SAD	SAD	DRG	SDE	LFT
d-o-f	Mag	Yaw	Pitch	Drag	Side	Lift
Recent NASA Configuration (M_z)						
Field			B_z	B_{xz}	B_{yz}	B_{zz}
Coils			LFT′ (++)	LFT′ (+–)	SAD′	DRG
d-o-f			Algn	Drag	Side	Lift
Present Configuration (M_z)						
Field	B_x	B_y	B_z	B_{xz}	B_{yz}	B_{zz}
Coils	MAG	SDE (rev)	LFT′ (++)	LFT′ (+–)	SAD′	DRG
d-o-f	Pitch	Roll	Algn	Drag	Side	Lift

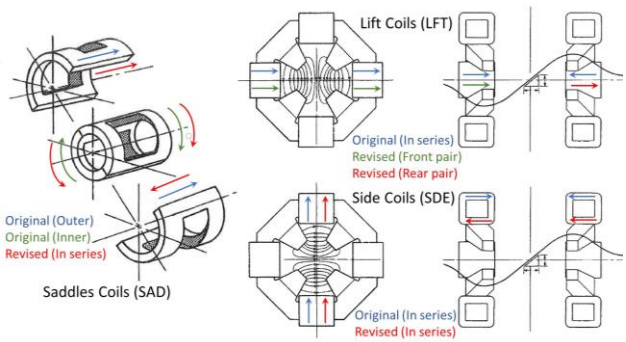

Figure 2 Revised electromagnet configuration

2.2 System Dynamics as a Function of Pressure

Prior analysis based on a framework originally developed by Groom [7] gives an indication of the challenge of raising dynamic pressure to the point where aerodynamic forces are many times the weight of the magnetically suspended model. Analysis is based on a linearized open-loop model with either axial or transverse magnetization. An idealized calculation is based on including the field gradients required to overcome model weight and drag only, with all second-order gradients set to zero. An alignment field is added for the current configuration, although this could be removed if full-authority control loops were functional in pitch and roll. Of interest is the largest magnitude of eigenvalues on the real axis (unstable) and the largest magnitude on the imaginary axis (oscillatory). Results are summarized in Table 2, all given in radians/sec. It is seen that the "compass needle" modes arising from the alignment field may be the most challenging to control. For reference, the reference model weight is around 0.5 N.

2.3 Upgrades to Permit Increased Dynamic Pressure

The passively stable axes (pitch and roll) have proved problematic, with oscillations at the modal frequency (order-of-magnitude 10-20 Hz) arising unpredictably. The decision was made to close the pitch and roll loops so as to provide some damping, along with a secondary advantage of being able to command non-zero orientations. This required that additional electromagnets be activated (Table 1) to provide transverse magnetic fields, plus the addition of pitch and roll attitude sensing.

Table 2 Largest eigenvalues for various configurations

Drag=0	1 N	2 N	Comments
MIT with M_z and alignment field			
±232.3i ±12.5	±232.3i ±18.0	±232.3i ±28.5	Compass needle mode
Original MIT configuration with M_x			
±36.7i ±36.7	±75.7i ±75.7	±105.9i ±105.9	
Notional MIT with alignment field zeroed			
±51.9i ±51.9	±62.3i ±62.3	±78.7i ±78.7	Requires closed loops on θ, ϕ

2.3.1 EPS Upgrades

With a magnetic core length-to-diameter ratio nominally unity, the output from the EPS in response to pitch rotation is very small. Electromagnetic asymmetry is required and can be introduced by adding a thin copper loop, initially oriented with its axis along the axis of the wind tunnel, resembling a dipole antenna (Figure 3). Large yaw angles are possible with the free-to-yaw configuration, so a second loop can be introduced with its output with changes of yaw orientation. The amplitudes of the EPS position outputs are greatly enhanced compared to the magnetic core alone, with pitch sensed via an additional EPS channel, in more-or-less the same way as originally conceived by MIT. Unfortunately, roll cannot be sensed without introducing significant further

Figure 3 EPS sensing loop within Stardust model

asymmetry, so the possibility of using optical sensing for roll was examined.

2.3.2 Motion Capture Cameras

A pair of OptiTrack™ Prime^{x}22 motion capture cameras were already being used to explore the possibility of a complete replacement of the EPS system. These cameras have a resolution of 2048×1088 pixels, a maximum frame rate of 360 Hz at full resolution and a latency (image acquisition to output) of 2.8 ms. On-camera processing is used to extract target positions in the camera frame of reference. In principle, OptiTrack "Motive" software will reconstruct the location and orientation of a 3D object equipped with multiple targets. Unfortunately, the limited optical access in this case

presents a serious challenge for full 6 d-o-f measurement, with further development required, but each camera can successfully track single or dual targets centered on the face of the model being viewed, with configuration carried out via an API. Two target pairs on opposite sides of the model, with cameras in the horizontal plane is sufficient to extract pitch and roll measurements. To minimize glare from the camera's integral IR LEDs, the viewing directions are slightly inclined, as illustrated in Figure 4.

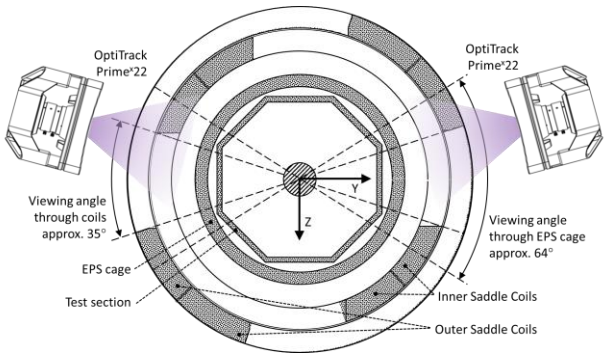

Fig. 4 Cross-section of the MSBS at the model location, showing optical access.

2.3.3 Control System

The control system implements a full state feedback LQR algorithm, with displacements derived from the EPS outputs (potentially also from the cameras), pitch and roll derived from the OptiTrack cameras (with EPS pitch available as an alternative) and all rates derived from a state estimator. The system is implemented in Simulink and executed on Speedgoat™ hardware. A progressive sequence of controllers is tuned for good behavior at different dynamic pressures, with the system switching between gain matrices as tunnel speed rises or falls. The system executes at a 1 kHz loop rate, with I/O at that rate aside from the cameras, which report asynchronously at their inherent rate, with the controller recovering the most recently available target locations. Three degree-of-freedom controllers (x, y, z translation) have been used extensively up to dynamic pressures of around 1 kPa, with pitch and roll made passively stiff by a steady vertical alignment field. It was found that as dynamic pressure was further increased the passive pitch

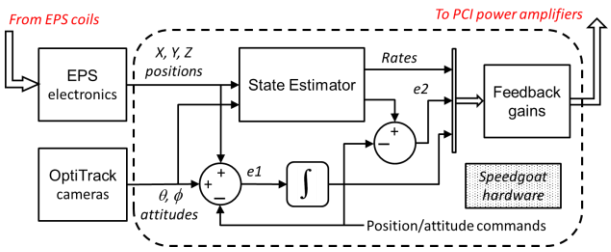

Figure 5 Controller block diagram

and roll modes would exhibit slight negative damping, with the mode shapes depending on model geometry, but often dominated by roll. It was concluded that four d-o-f control would offer little advantage, so attention was focused on the five d-o-f option, relying on camera information for the pitch and roll loops, with EPS outputs an alternative for pitch.

2.3.4 Wind Tunnel Calibration

A wind tunnel calibration was carried out as this had not been done since the original honeycomb was removed and the fan drive upgraded. A pitot rake was positioned slightly downstream of the model location, mounted corner-to-corner across the test section. The basic speed calibration compared well against the original [8]. The flow uniformity shows less than ±0.1% dynamic pressure variation across the core flow (Figure 6), although the boundary layers are quite thick, due to the unusually long test section. A TSI 1210-20 hot wire probe was then mounted at the test section centroid with turbulence measured over a range of speeds via a TSI IFA-300 anemometer with a Measurement Computing USB-1604 DAQ. Sample rates were 50 kHz, with 5 second data records. Figure 7 summarizes results, with a typical power spectrum shown in Figure 8. As reported by MIT, the overall turbulence intensity is dominated by low frequency components, thought to originate in the fan section.

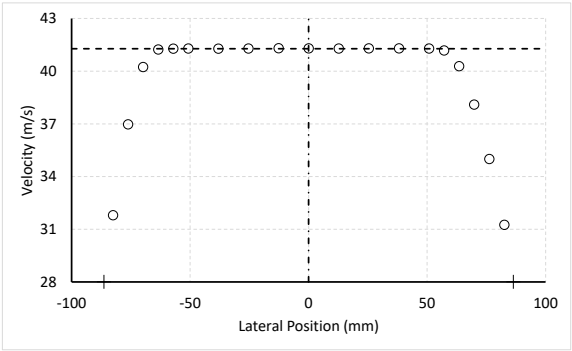

Figure 6 Flow uniformity, V=41.3 m/s

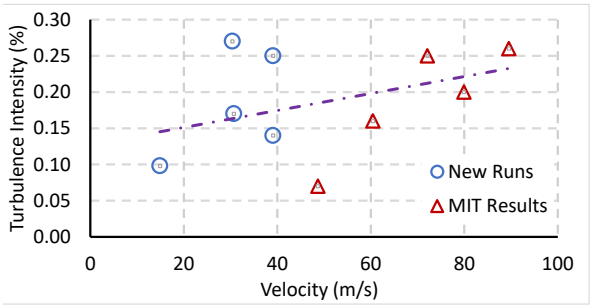

Figure 7 Turbulence intensity versus tunnel speed

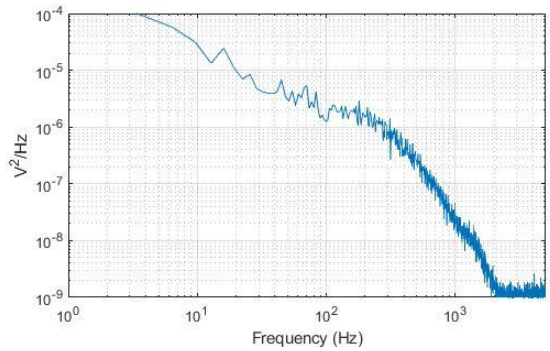

Figure 8 Turbulence Spectrum at q=935 Pa

3. Results and Discussion

All hardware changes discussed herein have been implemented with the commissioning process underway at the time of writing. It is anticipated that the pitch and roll control loops can provide damping of those degrees-of-freedom, permitting successful aerodynamic testing at progressively increasing dynamic pressures. The near-term objective is to double the prior limit for practical operation, up to a value of at least 2 kPa.

4. Concluding Remarks

The NASA/ODU MSBS continues to undergo extensive modifications and upgrades, focused on increasing the usable range of dynamic pressures. It is noted that the electromagnetic configuration does not resemble that of a new design, so the achievable q in the present facility is likely to be significantly lower than for a new design.

References

[1] Crane, J.F.W.: Air condensation effects at M=8.5 measured on the drag and the wake of a magnetically suspended 20 deg. cone. *ARC CP No.1177, 1970*

[2] Copeland, A.B., et.al.: Wind-Tunnel Measurement at M = 4.28 of Some Static and Dynamic Aerodynamic Characteristics of Finned Missiles Suspended Magnetically. *Journal of Spacecraft and Rockets, Vol. 5, No.7, July 1968*

[3] Takagi, Y., Sawada, H., Obayashi, S.: Development of Magnetic Suspension and Balance System for Intermittent Supersonic Wind Tunnels, *AIAA Journal, Vol.54, No.4, April 2016*

[4] Sevier, A.: Feasibility Study for Testing the Dynamic Stability of Blunt Bodies with a Magnetic Suspension System in a Supersonic Wind Tunnel. MS Thesis, Feasibility Study for Testing the Dynamic Stability of Blunt Bodies with a Magnetic Suspension System in a Supersonic Wind Tunnel, *MS Thesis, Case Western Reserve University, 2017*

[5] Stephens, T.: Design, Construction, and Evaluation of a Magnetic Suspension and Balance System for Wind Tunnels, *NASA CR-66903, November 1969*

[6] Britcher, C.P., Schoenenberger, M., Cox, D.: Demonstration of a Magnetic Suspension and Balance System with Transverse Magnetization, *ICFD 2019*

[7] Britcher, C.P.; Driver, D.; Cox, D.E.: Electromagnetic Modeling of Wind Tunnel Magnetic Suspension and Balance Systems. *AIAA SciTech Forum, January 23-27, 2023. AIAA 2023-1819*

[8] Vlajinac, M.: Design, Construction and Evaluation of a Subsonic Wind Tunnel. *MS Thesis, MIT, June 1970*